Journal of the Ceramic Society of Japan 105 [6] 504-508 (1997) Paper

Microstructural Stability of Si-Ti-C-O Fibers at High Temperatures

Ken-ichi KAKIMOTO,*† Toshio SHIMOO and Kiyohito OKAMURA

Department of Metallurgy and Materials Science, College of Engineering, Osaka Prefecture University, 1-1, Gakuen-cho, Sakai-shi, Osaka 593
**Graduate student, Osaka Prefecture University, 1-1, Gakuen-cho, Sakai-shi, Osaka 593*

高温環境下における Si-Ti-C-O 系繊維の微構造安定性

柿本健一*†・下尾聰夫・岡村清人

大阪府立大学工学部材料工学科，593 大阪府堺市学園町 1-1
*大阪府立大学大学院生，593 大阪府堺市学園町 1-1

The thermal stability of Si-Ti-C-O fibers, STC(6H) and STC(6) prepared by the pyrolysis of polytitanocarbosilane (PTC) was investigated. TEM study confirmed that STC(6H) contained larger β-SiC nanocrystals and higher crystalline free-carbon units than STC(6). During the exposure tests to high temperatures under Ar atmosphere, the crystallinity of the free carbon in STC(6H) further developed around β-SiC nanocrystals as if the free carbon formed nets for trapping β-SiC nanocrystals to prevent their direct contacts. STC(6H) showed slower gas-release and grain coarsening rates than STC(6). After being exposed at 1600°C for 60 min, STC(6H) retained the tensile strength of as high as 0.6 GPa, whereas STC(6) was too weak to handle for the tensile testing. The crystalline free-carbon had the excellent ability to retain the microstructural stability of Si-Ti-C-O fibers at high temperatures. [Received December 17, 1996; Accepted March 11, 1997]

Key-words : *Silicon-titanium-carbon-oxygen fiber (Tyranno fiber), TEM observation, Free-carbon, Gas release, Grain coarsening, Tensile strength*

1. Introduction

During the last quarter of a century great progress has been made in the development of high-performance ceramic matrix composites (CMCs) intended for use at high temperatures.[1),2)] One of the most important events that enabled this progress to come about was the development of polymer-derived Si-C-O fibers by Yajima et al.[3)] The Si-C-O fiber was made by melt-spinning of an organosilicon polymer (polycarbosilane) into a precursor fiber, followed by heating at an elevated temperature. Advantages of the polymeric route to ceramic fibers include the following: the ability to control fiber purity; the ability to control the crystallinity; and the ability to prepare continuous fibers with fine diameter suitable for weaving and knitting unobtainable by other traditional methods.[4)] Following the commercialization of the Si-C-O fiber (Nicalon; Nippon Carbon Co., Yokohama, Japan), polymer-derived Si-Ti-C-O fibers were produced by Ube Industries Ltd. (Ube, Japan) with the trade name Tyranno. The Si-Ti-C-O fiber has a fine diameter of 8 to 12 μm, high tensile strength of 2.8 to 3.0 GPa, and high Young's modulus of 200 to 220 GPa.[5)]

However, the Si-Ti-C-O fiber shows operation limits at high temperatures. Above 1300°C under Ar atmosphere, the Si-Ti-C-O fiber undergoes carbothermic reduction (loss of oxygen) known as the thermal decomposition reaction to produce CO and some SiO.[6),7)] Simultaneously, coarse β-SiC grains along with a small amount of TiC crystallites are formed. Such gas release and crystallization destroy the fiber structure, resulting in a remarkable decrease in the fiber strength.[6),8)] The limited thermal stability of Si-Ti-C-O fibers has been considered to be related with a large oxygen content (13-18 mass%).[7)] Most of the oxygen is incorporated during the curing process. The fiber is cured in air below 180°C by introducing chemical cross-links of oxygen atoms, because this treatment renders the fiber infusible so that its' shape will be retained during the next process known as the pyrolysis process. As far as the thermal oxidation curing is performed in the manufacturing process of the fiber, the fiber necessarily has a large oxygen content of 13-18 mass%; therefore, it has been expected that the oxidation curing method should be replaced by a new method. A main break-through concerns the curing of polycarbosilane fibers by Okamura et al.[9),10)] using γ-rays or electron beam irradiation under the presence of He gas. In this process, the cross-linkage between polymeric chains of the precursor was mainly achieved by forming Si-C bonds between polymeric chains, instead of Si-O-Si bridges as in the oxygen curing.

The electron-irradiation curing method permitted the preparation of the low oxygen grade (6 mass%) of the Si-Ti-C-O fiber. We reported that the gas release and the crystallization of the low oxygen grade at high temperatures proceeded fairly slowly, compared with those of conventional grades.[11)] In addition, we found that the thermal decomposition process of the Si-Ti-C-O fibers was controlled by the growth of β-SiC nanocrystals. Therefore, there is a possibility that the thermal stability of the fiber is affected strongly by not only its oxygen content but also its crystallinity. Generally, the fiber becomes microcrystalline from amorphous as the pyrolysis temperature for the preparation increases. In this study, two fiber specimens, which were prepared by different pyrolysis temperatures were, subjected to thermal exposure tests. This paper provides the information about the influence of the crystallinity of Si-Ti-C-O fibers on the thermal stability.

2. Experimental procedure

The fiber specimens used in this study were the low oxygen Si-Ti-C-O fibers, STC(6H) and STC(6), produced by Ube Industries Ltd. Their precursor fibers were derived from polytitanocarbosilane (PTC), and then were cured us-

† Now with Japan Science and Technology Corporation, Ceramics Superplasticity Project, Max-Planck-Institut für Metallforschung, Pulvermetallurgisches Laboratorium, Heisenbergstraße 5, 70569 Stuttgart, Germany
現在：科学技術振興事業団セラミックス超塑性プロジェクト，マックスプランク金属研究所粉末冶金研究室，Heisenbergstraße 5, 70569 Stuttgart, Germany

ing an electron beam accelerator at Takasaki Radiation Chemistry Research Establishment of Japan Atomic Energy Research Institute (JAERI; Takasaki, Japan). The irradiation curing was attained in He gas stream with an overall irradiation dose of 15 MGy. Subsequently, the cured fibers were subjected to a pyrolysis process at elevated temperatures under N_2 atmosphere after a preheating under Ar atmosphere. The final pyrolysis temperatures adopted for STC(6H) and STC(6) were 1500 and 1300°C, respectively. The chemical composition of the final products STC(6H) and STC(6) is given in Table 1. Both fibers have nearly identical composition, i.e., the oxygen content is approximately 6 mass%. Besides these low-oxygen grades, STC(13) and STC(18) containing oxygen of 13 and 18 mass%, respectively, were chosen to be reference fibers in this study.

The thermobalance for the experiment was composed of an analog-type automatic balance and a Tammann furnace. The graphite crucible (inside diameter: 26 mm, depth: 50 mm) containing 1 g of the fiber specimen was connected to the balance with rods made by stainless steel and graphite, and suspended in the constant-temperature zone of the furnace. The decrease in fiber mass by decomposition was continuously measured up to 60 min. The given temperatures were 1400, 1500, 1600 and 1700°C. The atmosphere in the furnace was Ar, which was let flow at a rate of 1.5×10^{-3} m^3/min from the furnace bottom. Upon completion of the measurement, the crucible was quickly moved upward into the upper section in the furnace to cool the specimen until it reached room temperature. The empty crucible was also heated in the same manner to find the blank value, by which the mass-loss curve was corrected.

The crystallinity of as-received and heat-treated fibers was determined by X-ray powder diffractometry (XRD) (Model RINT 1100, Rigaku, Tokyo, Japan) using Cu Kα radiation with a Ni-filter. Specifically, Auger electron spectroscopy detected that heat-treated fibers formed a thin carbon rich layer (max$<$30 nm) on the surface. For heat-treated fibers, therefore, the crystallinity of carbon phase which located near β-SiC grains was evaluated by using a transmission electron microscope (TEM) (Model JEM-2000FX, JEOL, Tokyo, Japan) to avoid the effect of the fiber surface; XRD was used not for the estimation of carbon crystallinity but for that of β-SiC grain size. TEM specimens were prepared by grinding fibers in ethanol, then a drop of the slurry was transferred to a copper grid, followed by vacuum drying. The microcrystallinity of fibers within a region of 350 nm diameter was determined by selected area diffraction (SAD). Dark-field (DF) images were used to examine the distribution of β-SiC grains in fibers. Lattice fringe (LF) techniques were used in order to describe the nanometer scale structure. The LF images were made by the interference among an incident beam and C_{002}- and/or β-SiC_{111}-scattered beams. Grain-boundary phases around β-SiC were analyzed by energy dispersive spectroscopy (EDS) (Model QX200J, LINK, Bucks, England). The tensile strength of fibers before and after heat-treatments was measured at room temperature by a monofilament method using a universal testing machine (Model Tensilon UTM-II-20, Orientec, Tokyo, Japan). The applied load, the gauge length and the crosshead speed were 100 g, 10 and 2 mm/min, respectively. Twenty specimens were tensile-tested in order to obtain an average value. The fractured surface of fibers was observed by a scanning electron microscope (SEM) (Model JSM-T20, JEOL, Tokyo, Japan).

Table 1. As-Received Si-Ti-C-O Fibers

Fiber	Pyrolysis Temperature (T/°C)	Chemical Composition
STC(6H)	1500	$SiTi_{0.03}C_{1.65}O_{0.17}$
STC(6)	1300	$SiTi_{0.02}C_{1.57}O_{0.21}$

3. Results and discussion

3.1 Microstructural stability

Figure 1 shows the XRD patterns of as-received STC(6H) and STC(6). The as-received specimens have broad patterns, indicating that they are microcrystalline. In comparison with STC(6), STC(6H) shows more distinct patterns which are centered at 2θ=36, 60 and 72°, each corresponding to β-SiC (111), (220) and (311), respectively. Corresponding to this result, TEM dark-field (DF) images from β-SiC reflections at (111) show that STC(6H) has larger β-SiC grains, which disperse over amorphous, than STC(6) (Fig. 2). The grain size of STC(6H) is of the order of 3-5 nm, while STC(6) reveals an amorphous-like state of fine grains less than 2 nm. The most noteworthy point is that STC(6H) alone shows a very weak reflection (a single arrow on the photo) besides the three rings due to β-SiC in the SAD pattern. The corresponding LF image also

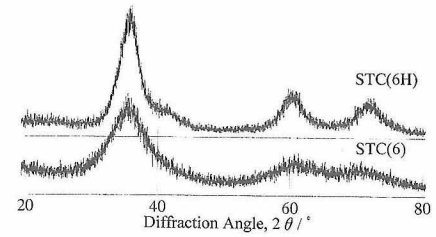

Fig. 1. XRD patterns of as-received STC(6H) and STC(6).

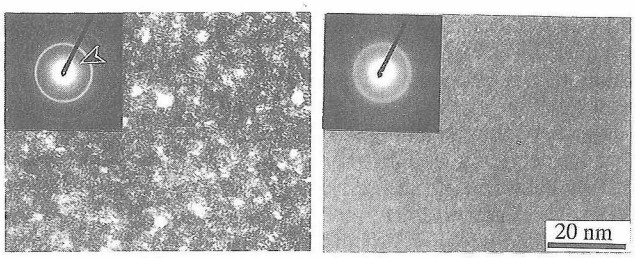

Fig. 2. TEM photographs (SAD (inset) and DF images) of as-received (a) STC(6H) and (b) STC(6). A single arrow on the SAD(a) indicates a C_{002} ring.

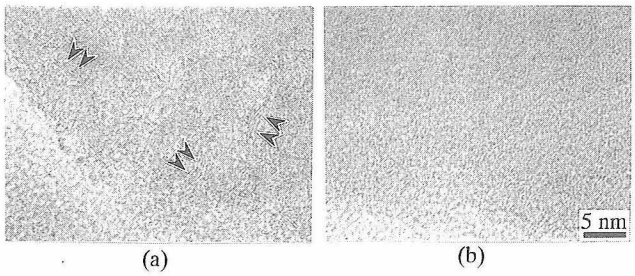

Fig. 3. TEM photographs (LF images) of as-received (a) STC(6H) and (b) STC(6). Double arrows on the photo(a) show free-carbon layers.

confirms very short stacks of three to five wrinkled fringes (d=0.347 nm, double arrows on the photo), as shown in Fig. 3(a). Each fringe corresponds to the projection of poly-aromatic carbon layers, in turbostratic order toward the (002) direction, which are commonly observed in other polymer-derived SiC materials such as Nicalon Si–C–O fibers too.[12] Most of the materials have C/Si atomic ratios higher than 1 due to the polymer composition and structure. Therefore, the occurrence of a "free carbon" phase could be expected after heat treatments; we previously confirmed that the Si–Ti–C–O fiber with a C/Si atomic ratio of 0.99 contained little free-carbon fringe, only having almost same size of β-SiC grains as STC(6H).[13]

The reason why the free-carbon layers of STC(6H) have such a curved structure can be explained by a speculation from the DF image of β-SiC_{111}, i.e., because they lie close to spherical β-SiC nanocrystals. On the other hand, STC(6) shows almost no C_{002} ring in the SAD pattern, only showing the weak diffuse rings due to β-SiC. The corresponding LF image also becomes a blur because of the weak scattered beams. According to SiC stoichiometric viewpoints, not only STC(6H) but also STC(6) should contain free carbon excess (Table 1). However, STC(6) did not show free carbon on the TEM photos, presumably because the free carbon was poor in crystallinity (amorphous) and thus the intensity in the SAD pattern was too low to be noticed. The wrinkled free-carbon layers observed in STC(6H) can be considered to be formed by thermal activation due to the higher pyrolysis temperature of STC(6H) than that of STC(6):

$$C_{free}\ (\text{amorphous}) \rightarrow C_{free}\ (\text{wrinkle}) \qquad (1)$$

In summary, STC(6H) contains larger β-SiC nanocrystals and higher crystalline free-carbon layers than STC(6), although both of the fibers have almost the same chemical composition.

Figure 4 compares the decomposition induced mass-loss curves of STC(6H) with those of STC(6) at 1500, 1600 and 1700°C. The mass-loss is considered to be caused by gas evolution of CO and SiO from the fibers.[7] STC(6H) has slower mass-loss rates than STC(6) at all test temperatures. At 1700°C, in particular, the two fibers demonstrate quite different mass-loss behaviors. The mass-loss of STC(6H) occurs constantly from the start, and it is not completed within 60 min, whereas STC(6) finishes the mass-loss in a short holding time of 28 min. This indicates that the onsetting rate of the decomposition is quite different between the two fibers. To investigate such differences from microscopic viewpoints, both STC(6H) and STC(6) were heat-treated at 1700°C for a short holding period of 10 min, then they were subjected to TEM analysis. The TEM photographs

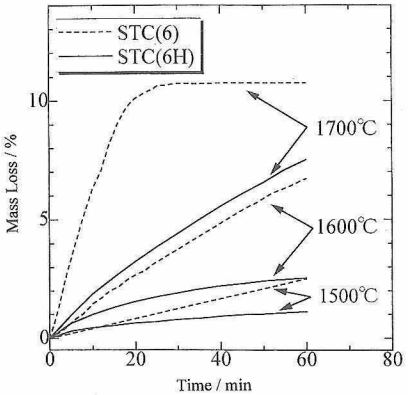

Fig. 4. Comparison of the mass-loss curves of STC(6H) with those of STC(6) at 1500, 1600 and 1700°C.

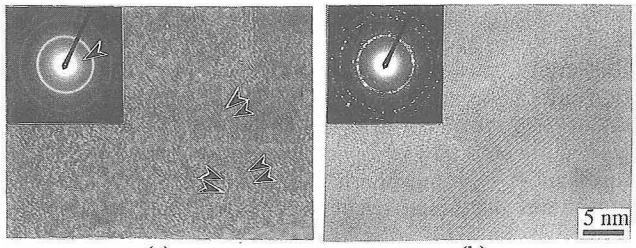

Fig. 5. TEM photographs (SAD (inset) and LF images) of (a) STC(6H) and (b) STC(6) heat-treated at 1700°C for a short period of 10 min. A single arrow and double arrows on the photos show a C_{002} ring and free-carbon layers, respectively.

are presented in Fig. 5. The C_{002} ring (a single arrow on the photo) of STC(6H) becomes more distinct than that of the as-received specimen. The corresponding free-carbon structure also changes in the form from some wrinkles into continuous networks (double arrows on the photo):

$$C_{free}\ (\text{wrinkle}) \rightarrow C_{free}\ (\text{network}) \qquad (2)$$

Such textural change (crystallization) of carbon has been commonly observed in carbonaceous materials with increasing heat-treatment temperature:[14] i.e., the adjacent basic columns of carbon became to get hooked to one another, edge to edge, forming the straight long-chained layers. However, the free carbon shown in Fig. 5(a) demonstrates no straight structures but curving structures, suggesting that the ordering (crystallization) of free carbon has occurred preferentially around the peripheral faces of β-SiC grains. Monthioux et al.[15] have reported on the polymer-derived SiC ceramics containing free carbon that the electrical conductivity increased exponentially with increasing heat-treatment temperature. This observation seems to result from the perfection of free-carbon networks which should be electrical conduction paths.

On the other hand, the heat-treated STC(6) demonstrates no free-carbon network but coarse β-SiC crystals (Fig. 5(b)). The SAD pattern also shows distinct spotty rings of β-SiC only. Figure 6 shows the average crystallite size of β-SiC in STC(6H) and STC(6) as a function of holding time at 1700°C. The size was calculated from their XRD data by using the Scherrer's equation. The calculated size of the β-SiC crystallite in STC(6) increases from 2 to 21 nm within a short holding time of 10 min. Finally, it reaches almost a saturated value of 33 nm in a holding time of 60 min, indicating that a rapid crystallization occurred.

For STC(6H) the crystallite size of β-SiC gradually in-

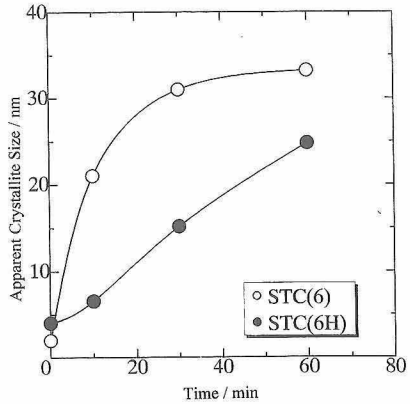

Fig. 6. Average crystallite size of β-SiC in STC(6H) and STC(6) heat-treated at 1700°C for 10, 30 and 60 min. These values were determined from their XRD data by using the Scherrer's equation.

creases at a constant rate with holding time. The value after a heat-treatment time of 60 min is 25 nm, which is close to the value of STC(6) after a holding time of 10 min, i.e., the crystallization of STC(6H) was retarded significantly. A noteworthy point is that such crystallization curves are very similar in the appearance to the mass-loss curves (Fig. 4). This indicates that there is a close relationship between the gas evolution behavior and the crystallization behavior in the decomposition process of Si–Ti–C–O fibers, as shown:

$$SiTi_xC_yO_z \rightarrow \beta\text{-SiC} + TiC + CO + SiO \quad (3)$$

But what makes the different decomposition behavior between STC(6H) and STC(6)? STC(6H) contains larger β-SiC nanocrystals and higher crystalline free-carbon in the as-received state than STC(6). The following effects are considered to be the answer against the above question:

(i) initial size of β-SiC nanocrystals

(ii) crystallinity of free-carbon

In the preceding paper,[13] we have reported that the Si–Ti–C–O fiber with little free-carbon demonstrated a severe thermal decomposition like STC(6), although the fiber had almost the same grain size of β-SiC as STC(6H). Rather than the parameter (i), therefore, the latter parameter (ii) seems to affect the fiber decomposition rate strongly. As shown in Fig. 3(a), as-received STC(6H) has already contained the highly crystalline free-carbon. Such highly crystalline free-carbon must have worked as an inhibitor against the abrupt crystallization of β-SiC. Based on TEM observation, the working mechanism is considered to be that the free carbon, first, formed nets around β-SiC nanocrystals in a short heating period, followed by trapping β-SiC nanocrystals to forbid their direct contacts (Fig. 5(a)). These processes seem to have resulted in the slow grain growth of β-SiC. Furthermore, the slow grain coarsening can lead to the slow gas release from the fiber. This is possibly associated with the fact that clear-cut grain boundaries are difficult to form during the slow grain coarsening, which can result in a slow progress of void formation required to work as paths for the gas release. Therefore, STC(6H) is considered to show a slower mass-loss behavior as well as a slower crystallization than STC(6), especially in the early holding period. However, the TEM observation confirmed that such carbon nets were not stable permanently but subsequently began to disappear with heat-treatment time after 10 min, presumably because the free carbon was gradually eliminated as CO gas during the fiber decomposition. β-SiC grains grew as the free-carbon nets disappeared.

Figure 7 presents the TEM photograph in the neighborhood of such a coarse β-SiC grain. EDS analysis was performed in a region perpendicular to the grain boundary of the β-SiC grain over amorphous. Ti-rich regions form around the β-SiC grain boundary, and they were found to be TiC from the XRD result. It has been reported that TiC does not form a solid solution with β-SiC.[16] Thus TiC seems to have accumulated around β-SiC grains as they grew intensively with heat-treatment time, which may have formed a well-conductive path in the fiber by the so-called percolation phenomenon.[15] In practice, it is possible that TiC around β-SiC grains has already existed in sub-nanometers scale for the fiber heat-treated for a shorter period than 10 min, in other words, it was not until the pronounced grain growth of β-SiC that TiC was noticed because of satisfying the resolution of EDS probes. Yamamura et al.[5] have observed that Si–Ti–C–O fibers retained its microcrystalline state up to higher temperatures by 100°C than no Ti-containing fibers which were prepared using the same procedure as the Si–Ti–C–O fibers. Therefore, TiC as well as free-carbon nets may have the ability to control β-SiC grain growth by hindering a direct contact between β-SiC grains. However, it has been reported on the Si–Ti–C–O fibers with high Ti contents that large TiC crystallites were formed and β-SiC grain growth also occurred quickly.[17),18] In this case, a significant amount of TiC may have acted as nucleation sites around individual β-SiC grains, thereby helping their rapid growth; further investigations on this point are being carried out.

3.2 Strength retention

The tensile strength of heat-treated STC(6H) and STC(6) was measured at room temperature to examine their strength retention after thermal decomposition. The fiber specimens heat-treated at temperatures from 1400 to 1700°C for 60 min were offered for the measurement. The tensile strength are shown in Fig. 8, including the result of the high oxygen grade fibers STC(13) and STC(18) too. Average tensile strengths of all the as-received fibers are nearly equal regardless of their different crystallinities and/or oxygen contents. However, their tensile strength decreases in different manners with increasing heat-treatment temperature. The same strength-retention level shifts upward approximately 100°C interval in the order STC(18,

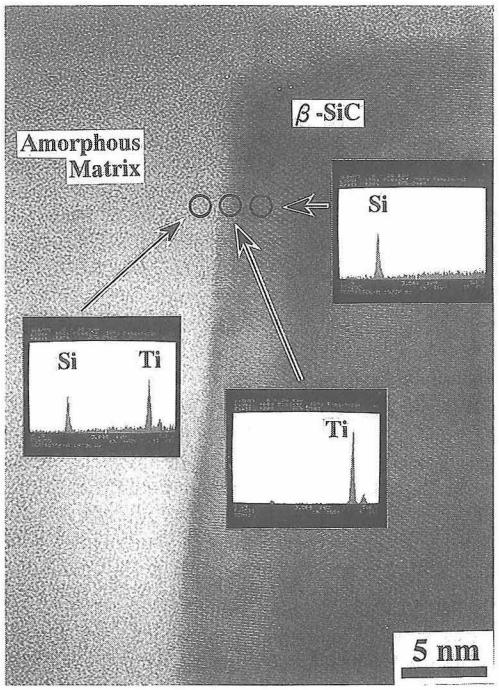

Fig. 7. TEM–EDS analysis of the grain boundary of a coarse β-SiC grain.

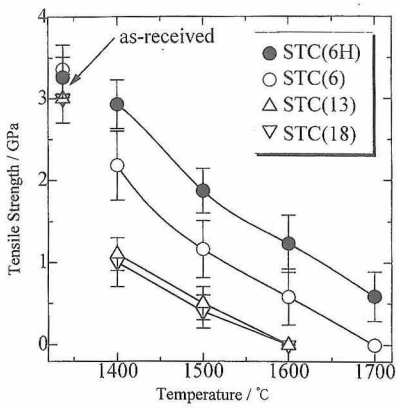

Fig. 8. Tensile strength of STC(6H) and STC(6) heat-treated at various temperatures for 60 min. The strength of the reference fibers, STC(13) and STC(18), is also shown.

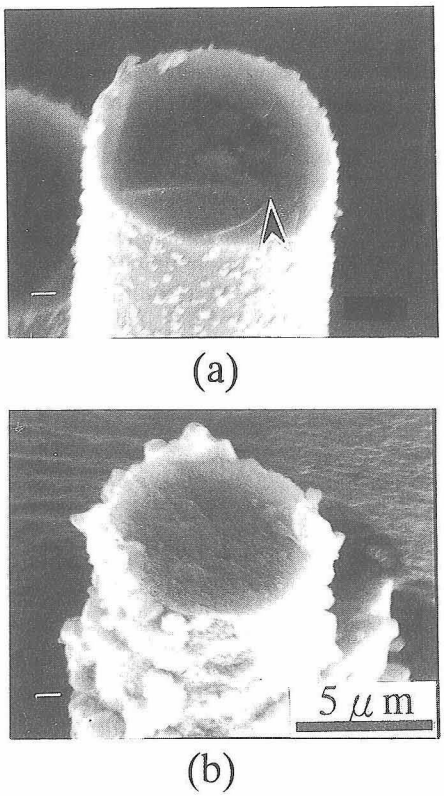

Fig. 9. SEM photographs of the surface and the fractured surface of (a) STC(6H) and (b) STC(6) heat-treated at 1600°C for 60 min.

13)<STC(6)<STC(6H). Both STC(6H) and STC(6) of low oxygen grades seem to have suffered less microstructural changes than STC(13) and STC(18) during the thermal exposure tests, since strength-controlling defects are caused by the release of oxygen-containing gases. Nevertheless, STC(6H) is found to be furthermore stronger than STC(6), although both fibers have almost the same oxygen content. No further strength measurement could be made on STC(6) heat-treated at 1700°C. By contrast, STC(6H) after held at 1700°C retains 18% (0.6 GPa) of its initial strength. This result reflects that the fiber crystallinity as well as the oxygen content is a very important factor for the microstructural stability resulted in the strength retention. Figure 9 presents the typical SEM photographs of the surface and the fractured surface of STC(6H) and STC(6) heat-treated at 1600°C for 60 min. STC(6H) exhibits a mirror fracture, indicating that the place indicated by an arrow on the photo was the starting point of fracture. The fiber retains a tensile strength as strong as 38% of the initial strength (Fig. 8). On the other hand, STC(6) exhibits no well-defined mirrors but a severe grain coarsening of β-SiC both along the surface (granular precipitates are presumed to be formed by the reaction of SiO gas with C) and the fractured surface, although as-received STC(6) as well as STC(6H) revealed a similar featureless smooth surface. The starting point of the fracture can be hardly presumed. The tensile strength retains only 17% of the initial value. The heat-treated STC(6) must have contained a lot of flaws, which determined the low tensile strength, due to the less thermal stability.

4. Conclusions

The microstructural stability at high temperatures of polytitanocarbosilane-derived Si-Ti-C-O fibers, STC(6H) and STC(6), has been investigated. STC(6H) was prepared at a higher pyrolysis temperature at 1500°C than STC(6) at 200°C. STC(6H) contained larger β-SiC nanocrystals and higher crystalline free-carbon than STC(6), although both of them had almost the same chemical composition. STC(6H) showed a much slower crystallization rate and had a smaller gas-release rate than STC(6) during heat treatments beyond 1400°C. STC(6H) also exhibited a higher retention in the tensile strength than STC(6). The TEM analysis on STC(6H) confirmed that the crystallinity of the free-carbon units was further enhanced, and they formed networks around β-SiC nanocrystals within a short heat-treatment time. The free-carbon behaved as if they were obstacles against the grain growth of β-SiC. Such free-carbon texture seems to be the main reason for the good thermal stability of STC(6H). Thermal stability of polymer-derived Si-C system fibers has been discussed only in terms of the oxygen content. However, the present study let us expect that the thermal stability of Si-Ti-C-O fibers can be improved not only by lowering the oxygen content but also by the microstructural modification, that is, by making crystalline free-carbon units which work as an inhibitor against the grain coarsening of the fibers.

Acknowledgments The authors are very grateful to Ube Industries Ltd., for the supply of samples and chemical analysis, and to Dr. Seguchi (JAERI) for his help with the electron beam curing. This work was supported by a great from the Nippon Sheet Glass Foundation for Materials and Engineering.

References

1) L. M. Sheppard, *Am. Ceram. Soc. Bull.*, **69**, 666-73 (1990).
2) R. Raj, *J. Am. Ceram. Soc.*, **76**, 2147-74 (1993).
3) S. Yajima, J. Hayashi, M. Omori and K. Okamura, *Nature*, **261**, 683 (1976).
4) J. Lipowitz, *Am. Ceram. Soc. Bull.*, **70**, 1888-94 (1991).
5) T. Yamamura, T. Ishikawa, M. Shibuya and K. Okamura, *J. Mater. Sci.*, **23**, 2589-94 (1988).
6) D. J. Pysher, K. C. Goretta, R. S. Hodder, Jr. and R. E. Tressler, *J. Am. Ceram. Soc.*, **72**, 284-88 (1989).
7) T. Shimoo, M. Sugimoto, Y. Kakehi and K. Okamura, *J. Japan Inst. Metals*, **55**, 294-303 (1991).
8) B. A. Bender, J. S. Wallace and D. J. Schrodt, *J. Mater. Sci.*, **26**, 970-76 (1991).
9) K. Okamura, M. Sato, T. Seguchi and S. Kawanishi, *J. Japan Soc. Powder and Powder Metallurgy*, **35**, 170-73 (1988).
10) K. Okamura and T. Seguchi, *J. Inorganic and Organometallic Polym.*, **2**, 171-79 (1992).
11) K. Kakimoto, T. Shimoo, K. Okamura, T. Seguchi, M. Sato, K. Kumagawa and T. Yamamura, *J. Japan Inst. Metals*, **58**, 229-34 (1994).
12) Y. Maniette and A. Oberlin, *J. Mater. Sci.*, **24**, 3361-70 (1989).
13) K. Kakimoto, T. Shimoo and K. Okamura, *Mater. Sci. Eng.*, **A217/218**, 211-14 (1996).
14) A. Oberlin, *Carbon*, **22**, 521-41 (1984).
15) M. Monthioux, A. Oberlin and E. Bouillon, *Compos. Sci. Technol.*, **37**, 21-35 (1990).
16) C. E. Bruckl, "Ternary Phase Equilibria in Transition Boron-Carbon-Silicon Systems, Part II, Vol. 7, AFML-TR-65-2," Ed. by Air Force Laboratory, Wright Patterson Air Force Base, OH (1966).
17) F. Babonneau, G. D. Soraru and J. D. Mackenzie, *J. Mater. Sci.*, **25**, 3664-70 (1990).
18) Y. Hasegawa, C. Feng, Y. Song and Z. Tan, *J. Mater. Sci.*, **26**, 3657-64 (1991).